Inorg. Chem. **2004**, *43*, 2703–2707

$[C_6N_2H_{14}]0.5\cdot[MnAl_3(PO_4)_4(H_2O)_2]$: A Manganese(II)-Substituted Aluminophosphate with AFN Topology

Lei Shi, Jiyang Li, Jihong Yu,* Yi Li, Hong Ding, and Ruren Xu*

State Key Lab of Inorganic Synthesis and Preparative Chemistry, College of Chemistry, Jilin University, Changchun 130023, P. R. China

Received November 18, 2003

A new manganese(II)-substituted aluminophosphate, $[C_6N_2H_{14}]0.5\cdot[MnAl_3(PO_4)_4(H_2O)_2]$, denoted as MnAPO-14, has been synthesized hydrothermally in the presence of 1,4-diazabicyclo[2.2.2]octane (DABCO) as the structure-directing agent. Its structure is determined by single-crystal X-ray diffraction analysis and further characterized by X-ray powder diffraction, ICP, and TG analyses. The structure of MnAPO-14 is built up by $MnO_4(H_2O)_2$ octahedra, AlO_4 tetrahedra, and PO_4 tetrahedra via Al–O–P and Mn–O–P linkages. Its framework is analogous to that of aluminophosphate zeotype AFN in which 25% of the aluminum sites are replaced by Mn(II) atoms. The diprotonated DABCO cations reside in the eight-membered ring channels. Computational simulations indicate that the substitution site of Mn to Al is determined by the host–guest interaction. Crystal data: $[C_6N_2H_{14}]0.5\cdot[MnAl_3(PO_4)_4(H_2O)_2]$, triclinic $P\bar{1}$ (No. 2), $a = 9.5121(4)$ Å, $b = 9.8819(3)$ Å, $c = 12.1172(4)$ Å, $\alpha = 70.533(2)°$, $\beta = 73.473(2)°$, $\gamma = 82.328(2)°$, $Z = 2$, $R_1 = 0.0586$ ($I > 2\sigma(I)$), and $wR_2 = 0.1877$ (all data).

Introduction

The synthesis of the alumimophosphate family of molecular sieves ($AlPO_4$-*n* where *n* denotes the structure type) was first reported by Wilson et al. in 1982.[1] These materials are typically built up from strict alternation of AlO_4 and PO_4 tetrahedra forming a neutral open framework. So far, over 30 types of aluminophosphate zeotype structures have been reported,[2] such as $AlPO_4$-5 (AFI),[3] AlPO-11 (AEL),[4] and VPI-5 (VFI),[5] etc. The isomorphic substitution of catalytically active transition metal ions, such as Ni(II), Pd(II), Mn(II), Fe(III), V(II), or Co(II), into framework sites of aluminophosphate zeotypes has been successfully applied in catalysis where aerial oxidations are possible using linear and cyclic hydrocarbons.[6] In addition, ethylene dimerization can be catalyzed by incorporation of Ni(II) or Pd(II) into aluminophosphates;[7] MeAPOs (Me = Fe, Co, Mn) have significant catalytic activities for the hydroxylation of phenol with hydrogen peroxide;[8] nickel-containing SAPO-34 is one of the best catalysts for methanol to olefin (MTO) conversion yielding close to 90% ethene at a reaction temperature of 450 °C.[9]

The incorporation of Mn into aluminophosphate zeotypes, such as $AlPO_4$-5, $AlPO_4$-11, $AlPO_4$-34, and $AlPO_4$-41, has been widely studied in the literature. However, the isomorphous substitution of framework Al by large amounts of Mn is normally difficult to achieve. Brouet et al. reported direct ESEM evidence for Al substitution at a low Mn content (0.1 mol %) in MnAPO-11 and MnSAPO-11,[10] whereas Goldfarb et al. concluded, using ESR methods, that MnAPO-5, for the most part, did not isomorphically substitute framework Al atoms despite that a certain amount of Mn atoms were

* Authors to whom correspondence should be addressed. E-mail: jihong@mail.jlu.edu.cn.

(1) Wilson, S. T.; Lok, B. M. C.; Messina, A.; Cannan, T. R.; Flanigen, E. M. *J. Am. Chem. Soc.* **1982**, *104*, 1146.
(2) Baerlocher, Ch.; Meier, W. M.; Olson, D. H., Eds.; *Atlas of Zeolite Framework Types*; Eslevier: London, 2001.
(3) Bennett, J. M.; Cohen, J. P.; Flanigen, E. M.; Pluth, J. J.; Smith, J. V. *ACS Symp. Ser*. **1983**, *218*, 109.
(4) Bennett, J. M.; Richardson, J. W., Jr.; Pluth, J. J.; Smith, J. V. *Zeolites* **1987**, *7*, 160.
(5) Davis, M. E.; Saldarriaga, C.; Montes, C.; Garces, J.; Crowder, C. *Nature* **1988**, *331*, 698.
(6) Hartmann, M.; Kevan, L. *Chem. Rev.* **1999**, *99*, 635.
(7) (a) Hartmann, M.; Kevan, L. *J. Chem. Soc., Faraday Trans*. **1996**, *92*, 1429. (b) Hartmann, M.; Kevan, L. *J. Phys. Chem.* **1996**, *100*, 4606.
(8) Dai, P. S. E.; Petty, R. H.; Ingram, C. W.; Szostak, R. *Appl. Catal. A* **1996**, *143*, 101.
(9) Thomas, J. M.; Xu, Y.; Catlow, C. R. R.; Couves, J. W. *Chem. Mater*. **1991**, *3*, 667.
(10) (a) Brouet, G.; Chen, X.; Kevan, L. *J. Phys. Chem*. **1991**, *95*, 4928. (b) Brouet, G.; Chen, X.; Kevan, L.; Lee, C. W. *J. Am. Chem. Soc*. **1992**, *114*, 3770. (c) Lee, C. W.; Chen, X.; Kevan, L. *J. Phys. Chem*. **1992**, *96*, 3110. (d) Pluth, J. J.; Smith, V.; Richardson, J. W., Jr. *J. Phys. Chem*. **1988**, *92*, 2734.

10.1021/ic035329a CCC: $27.50
Published on Web 03/18/2004

involved in the product.[11] Recently, Stucky and co-workers were able to increase the substitution degree by applying a novel synthesis route on the basis of host−guest charge-density matching principle.[12] It is reported that Mn(II) atoms in the aluminophosphate zeotypes, such as MnAPO-11[4] and MnAPO-50,[13] are tetrahedrally coordinated in the framework. However, the Mn sites cannot be unambiguously determined by single-crystal X-ray diffraction analysis.

$AlPO_4$-14 built up from alternation of AlO_n polyhedra (AlO_4, $AlO_4(OH)$, and $AlO_5(OH)$) and PO_4 tetrahedra has a zeotype of AFN with eight-membered ring channels.[14] There have been reports on its gallophosphate analogue GaPO-14[15] and Cr-substituted analogue CrAPO-14[16] in which 4−5% of the alumina in the six-coordinated sites are substituted by Cr atoms. However, there is no report on Mn-substituted AlPO-14. In this work, we report the manganese(II)-substituted aluminophosphate zeotype AFN in which the substitution of Mn to Al is up to 25%. Its synthesis and structure have been studied. The isomorphic substitution of Mn(II) to Al sites in AFN has been investigated by computer simulations.

Experimental Section

Synthesis and Characterization. MnAPO-14 was prepared under hydrothermal conditions. Manganese chloride tetrahydrate and aluminum triisopropoxide were first dispersed into distilled water, followed by addition of DABCO. The mixture was stirred for 30 min and the orthophosphoric acid (85 wt %) was added to give a gel with overall composition of $MnCl_2{\cdot}4H_2O/Al(^iPrO)_3/H_3PO_4$/DABCO/$H_2O$ 1.2:1.0:4.0:4.0:500. The gel was stirred until it was homogeneous, sealed in a Teflon-lined stainless steel autoclave, and heated at 180 °C for 6 days under static conditions. The final product consisting of light pink, prism-like crystals was separated by sonication, and then washed with distilled water and dried in air at room temperature. X-ray powder diffraction (XRD) data were collected on a Siemens D5005 diffractometer with Cu Kα radiation (λ = 1.5418 Å).

Inductively coupled plasma (ICP) analysis was performed on a Perkin-Elmer Optima 3300Dv spectrometer. Elemental analyses were conducted on a Perkin-Elmer 2400 elemental analyzer. Thermogravimetric analysis (TGA) was carried out on a Perkin-Elmer TGA 7 unit in air with a heating rate of 20 °C/min.

Structure Determination. A suitable single crystal of dimensions 0.40 × 0.23 × 0.21 mm^3 was selected for single-crystal X-ray diffraction analysis. The data were collected on a Siemens SMART CCD diffractometer using graphite-monochromated Mo Kα radiation (λ = 0.71073 Å) at a temperature of 20±2 °C. Data processing was accomplished with the SAINT processing program.[17] Direct methods were used to solve the structure using the SHELXL crystallographic software package.[18] The Mn, Al, and P atoms could be unambiguously located, and the C and N atoms were subsequently located from difference Fourier map. Diprotonation of DABCO molecules with an occupancy of 0.5 was suggested by charge balance, as well as elemental and TG analyses. The hydrogen atoms in DABCO molecules were placed geometrically and refined in a riding model. H atoms associated with the water molecules coordinated to Mn atoms were not added. All non-hydrogen atoms were refined anisotropically. Structure details and selected bond lengths and distances are listed in Tables 1 and 2, respectively.

Table 1. Crystal Data and Structure Refinement for MnAPO-14[a]

empirical formula	$C_3\ H_{11}\ Al_3\ Mn\ N\ O_{18}\ P_4$
fw	608.89
temp	293(2) K
wavelength	0.71073 A
cryst syst, space group	triclinic, $P\bar{1}$
unit cell dimensions	a = 9.5121(6) Å; α = 70.533(4)°
	b = 9.8819(6) Å; β = 73.473(4)°
	c = 12.1172(7) Å; γ = 82.328(4) °
volume	1028.57(11) Å^3
Z, calcd density	2, 1.966 Mg/m^3
abs coeff	1.165 mm^{-1}
F(000)	608
cryst size	0.40 × 0.23 × 0.21 mm^3
theta range for data collection	1.84 to 24.99 °
limiting indices	$-9 \le h \le -11$, $-9 \le k \le 11$, $-13 \le l \le 14$
reflns collected/unique	5721/3605 [R(int) = 0.0484]
completeness to theta = 24.99	99.3%
abs correction	none
refinement method	full-matrix least-squares on F^2
data/restraints/parameters	3605/0/265
goodness-of-fit on F^2	1.046
final R indices [$I > 2\sigma(I)$]	R_1 = 0.0586, wR_2 = 0.1693
R indices (all data)	R_1 = 0.0794, wR_2 = 0.1877
largest diff. peak and hole	1.588 and −0.683 e.A^{-3}

[a] $R_1 = \sum(\Delta F/\sum(F_o))$; w$R_2$=$(\sum[w(F_o^2 - F_c^2)])/\sum[w(F_o^2)^2]^{1/2}$, w=$1/\sigma^2(F_o^2)$.

Simulation Method. The simulations were carried out in the Cerius^2 Package[19] by using Burchart1.01-Dreiding 2.21force field.[20] The energy terms associated with Mn(II) species were not given in this force field, so some parameters of bond energy for Mn−O were added according to the reported structures of MnAPOs: *Ro* = 2.12 Å and *Do* = 109.76 kcal/mol. The hypothetical structural models with $MnO_4(H_2O)_2$ in different substitution sites were built up from the AFN structure, in which an individual tetrahedrally coordinated Al site was replaced by Mn^{2+} followed by adding two H_2O molecules in a *cis* position in the octahedron. Energy minimization was performed to optimize the structural models upon keeping the symmetry of $P\bar{1}$ unchanged and relaxing the unit cell. The framework energy (E_f) and the interaction energy (E_{inter}) of host−guest were studied. The Coulombic interaction energy of the host−guest was ignored during the calculation.

Results and Discussion

Synthesis of the MnAPO-14. Pure single crystals of MnAPO-14 can be prepared in an aqueous system with the gel compositions of (0.5−1.5):1.0:4.0:4.0:500 $MnCl_2{\cdot}4H_2O/Al(^iPrO)_3/H_3PO_4$/DABCO/$H_2O$ at 180 °C for 6 days. It is

(11) Goldfarb, D. *Zeolites* **1989**, *9*, 509. Levi, Z.; Raitsimring, A. M.; Goldfarb, D. *J. Phys. Chem.* **1991**, *95*, 7830.
(12) (a) Feng, P.; Bu, X.; Stucky, G. D. *Nature* **1997**, *388*, 735. (b) Bu, X.; Feng, P.; Stucky, G. D. *Science* **1997**, *278*, 2080.
(13) Yušar, N. N.; Ristić, A.; Meden, A.; Kaučič, V. *Microporous Mesoporous Mater.* **2000**, *37*, 303.
(14) (a) Pluth, J. J.; Smith, J. V. *Acta Crystallogr.* **1987**, *C43*, 866−870. (b) Broach, R. W.; Wilson, S. T.; Kirchner, R. M. In *Proceedings of the 12th International Zeolite Conference*; Materials Research Society: Warrendale, PA, 1999; vol. III, p 1715.
(15) Parise, J. B. *Acta Crystallogr.* **1986**, *C42*, 670.
(16) Helliwell, M. *Acta Crystallogr.* **1993**, *B49*, 413.
(17) SMART and SAINT software packages; Siemens Analytical X-ray Instruments, Inc.: Madison, WI, 1996.
(18) Sheldrick, G. M. *SHELXL Program*, version 5.1; Siemens Industrial Automation, Inc.: Madison, WI, 1997.
(19) *Cerius2*; Molecular Simulations/Biosym Corporation: San Diego, CA, 1995.
(20) de Vos Burchart, E. Studies on Zeolite; Molecular Mechanics, Framework Stability and Crystal Growth. Ph.D. Thesis, Technische Universiteit Delft, 1992. de Vos Burchart, E.; van Bekkum, H.; van de Graaf, B.; Vogt, E. T. C. *J. Chem. Soc., Faraday Trans.* **1992**, *88*, 2761.

Table 2. Selected Bond Lengths [Å] and Angles [°] for MnAPO-14[a]

Mn(1)−O(11)	2.101(5)	Mn(1)−O(18)	2.117(4)
Mn(1)−O(6)	2.143(5)	Mn(1)−O(16)	2.239(5)
Mn(1)−O(13)	2.259(5)	Mn(1)−O(10)	2.291(5)
Al(1)−O(3)#1	1.724(5)	Al(1)−O(8)	1.730(5)
Al(1)−O(2)	1.742(5)	Al(1)−O(7)#2	1.757(5)
Al(2)−O(4)#3	1.728(5)	Al(2)−O(17)	1.732(5)
Al(2)−O(14)#4	1.742(5)	Al(2)−O(15)	1.755(5)
Al(3)−O(1)#5	1.718(5)	Al(3)−O(12)	1.725(5)
Al(3)−O(5)#2	1.739(5)	Al(3)−O(9)	1.743(5)
P(1)−O(6)#6	1.489(5)	P(1)−O(1)	1.529(5)
P(1)−O(9)	1.533(5)	P(1)−O(4)	1.543(5)
P(2)−O(18)	1.491(5)	P(2)−O(8)	1.529(5)
P(2)−O(7)	1.537(5)	P(2)−O(5)	1.537(5)
P(3)−O(16)	1.500(5)	P(3)−O(12)	1.527(5)
P(3)−O(2)	1.529(5)	P(3)−O(17)	1.538(5)
P(4)−O(11)	1.486(5)	P(4)−O(3)	1.526(5)
P(4)−O(14)	1.541(5)	P(4)−O(15)	1.555(5)
O(11)−Mn(1)−O(18)	92.7(2)	O(11)−Mn(1)−O(6)	90.8(2)
O(18)−Mn(1)−O(6)	93.06(19)	O(11)−Mn(1)−O(16)	89.09(19)
O(18)−Mn(1)−O(16)	97.87(18)	O(6)−Mn(1)−O(16)	169.07(19)
O(11)−Mn(1)−O(13)	102.4(2)	O(18)−Mn(1)−O(13)	164.90(19)
O(6)−Mn(1)−O(13)	88.28(19)	O(16)−Mn(1)−O(13)	81.08(18)
O(11)−Mn(1)−O(10)	173.0(2)	O(18)−Mn(1)−O(10)	82.76(19)
O(6)−Mn(1)−O(10)	94.7(2)	O(16)−Mn(1)−O(10)	86.33(18)
O(13)−Mn(1)−O(10)	82.15(18)	O(3)#1−Al(1)−O(8)	114.3(2)
O(3)#1−Al(1)−O(2)	107.3(3)	O(8)−Al(1)−O(2)	116.6(3)
O(3)#1−Al(1)−O(7)#2	104.0(3)	O(8)−Al(1)−O(7)#2	105.9(3)
O(2)−Al(1)−O(7)#2	107.8(3)	O(4)#3−Al(2)−O(17)	107.2(2)
O(4)#3−Al(2)−O(14)#4	111.0(3)	O(17)−Al(2)−O(14)#4	109.4(2)
O(4)#3−Al(2)−O(15)	106.6(2)	O(17)−Al(2)−O(15)	112.8(2)
O(14)#4−Al(2)−O(15)	109.8(2)	O(1)#5−Al(3)−O(12)	113.0(3)
O(1)#5−Al(3)−O(5)#2	106.7(3)	O(12)−Al(3)−O(5)#2	110.7(3)
O(1)#5−Al(3)−O(9)	110.5(2)	O(12)−Al(3)−O(9)	108.9(3)
O(5)#2−Al(3)−O(9)	106.9(2)	O(6)#6−P(1)−O(1)	112.9(3)
O(6)#6−P(1)−O(9)	111.4(3)	O(1)−P(1)−O(9)	108.4(3)
O(6)#6−P(1)−O(4)	112.5(3)	O(1)−P(1)−O(4)	106.3(3)
O(9)−P(1)−O(4)	105.0(3)	O(18)−P(2)−O(8)	113.5(3)
O(18)−P(2)−O(7)	110.7(3)	O(8)−P(2)−O(7)	108.3(3)
O(18)−P(2)−O(5)	109.5(3)	O(8)−P(2)−O(5)	106.5(3)
O(7)−P(2)−O(5)	108.2(3)	O(16)−P(3)−O(12)	110.3(3)
O(16)−P(3)−O(2)	112.0(3)	O(12)−P(3)−O(2)	108.2(3)
O(16)−P(3)−O(17)	113.5(3)	O(12)−P(3)−O(17)	106.1(3)
O(2)−P(3)−O(17)	106.4(3)	O(11)−P(4)−O(3)	113.0(3)
O(11)−P(4)−O(14)	112.4(3)	O(3)−P(4)−O(14)	106.3(3)
O(11)−P(4)−O(15)	111.0(3)	O(3)−P(4)−O(15)	106.8(3)
O(14)−P(4)−O(15)	107.1(3)	P(1)−O(1)−Al(3)#5	163.9(5)
P(3)−O(2)−Al(1)	143.1(3)	P(4)−O(3)−Al(1)#1	153.2(3)
P(1)−O(4)−Al(2)#3	143.4(3)	P(2)−O(5)−Al(3)#2	146.0(3)
P(1)#7−O(6)−Mn(1)	142.1(3)	P(2)−O(7)−Al(1)#2	141.2(3)
P(2)−O(8)−Al(1)	147.7(3)	P(1)−O(9)−Al(3)	145.7(3)
P(4)−O(11)−Mn(1)	158.8(3)	P(3)−O(12)−Al(3)	156.3(4)
P(4)−O(14)−Al(2)#4	135.9(3)	P(4)−O(15)−Al(2)	131.2(3)
P(3)−O(16)−Mn(1)	136.9(3)	P(3)−O(17)−Al(2)	149.8(3)
P(2)−O(18)−Mn(1)	137.1(3)	C(1)−N(1)−C(2)	108.4(16)
H-bond			
	N···N/Å	N−H···N/°	
N(2)−H(2)···N(2)#10	2.74(4)	171.3	

[a] Symmetry transformations used to generate equivalent atoms: (#1) $-x+1, -y, -z+1$; (#2) $-x, -y, -z+1$; (#3) $-x+1, -y+1, -z$; (#4) $-x+1, -y+1, -z+1$; (#5) $-x, -y+1, -z$; (#6) $x, y, z-1$; (#7) $x, y, z+1$.

found that many factors influence the synthesis of MnAPO-14, as shown in Table 3. When the molar ratio of Mn/Al is lower than 0.5 or higher than 1.5 in the gel, the dense phase of manganese phosphate can form easily. ICP analysis shows that the Mn/Al ratio stays as 1/3 in the products independent of the amount of Mn added in the initial gel.

The pH value is an important factor for the synthesis of MnAPO-14, and the optimum one is 8. If the pH value is higher than 8, the crystallinity of MnAPO-14 decreases, and when the pH value is higher than 10, the amorphous phase

Table 3. Synthesis Conditions and Resulting Products

sample code	gel composition (molar ratio)[a] MnO	Al_2O_3	P_2O_5	DABCO	pH	product
1	0.2−0.5	0.5	2	4	8	dense phase
2	0.6	0.5	2	4	8	MnAPO-14
3	0.8	0.5	2	4	8	MnAPO-14
4	1.0	0.5	2	4	8	MnAPO-14
5	1.2	0.5	2	4	8	MnAPO-14
6	1.2	0.5	2	4	8	MnAPO-14
7	1.5−2.5	0.5	2	4	8	dense phase
8	1.2	0.5	2	1−3	3−6	dense phase
9	1.2	0.5	2	3−4	7	MnAPO-14
10	1.2	0.5	2	4−8	8−10	impure MnAPO-14
11	1.2	0.5	2	9−12	10−11	amorphous phase

[a] Solvent = 500 H_2O; reaction temperature = 180 °C; reaction time = 6 days.

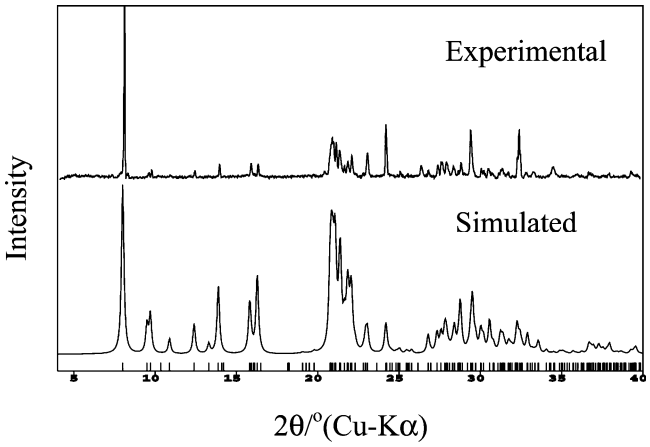

Figure 1. Experimental and simulated X-ray diffraction patterns of MnAPO-14.

is formed. On the other hand, if the pH is lower than 6, the dense phase of manganese phosphate is crystallized.

The type of solvent also influences the crystallization of MnAPO-14. When ethylene glycol, tetraethylene glycol, or 2-butanol is used as the solvent, keeping other conditions unchanged, no MnAPO-14 is formed, whereas when water and 2-butanol are used as a mixture of solvent, impure phase of MnAPO-14 is produced.

Figure 1 shows the experimental and simulated powder X-ray diffraction patterns of MnAPO-14, which are in good agreement with each other, suggesting the phase purity of the as-synthesized product.

ICP analysis gives the contents of Al, Mn, and P as 8.2, 8.9, and 20.3 wt %, respectively (calcd: Al, 8.32; Mn, 8.97; P, 20.23 wt %), leading to the (Al + Mn)/P ratio of 1. Elemental analysis gives the contents of C, N, and H as 2.93, 1.18, and 1.04 wt %, respectively (calcd: C, 2.95; N, 1.14; H, 1.06 wt %). The compositional analysis results are in agreement with the empirical formula $[MnAl_3(PO_4)_4(H_2O)_2]\cdot 0.5[C_6N_2H_{14}]$ given by single-crystal structure analysis.

The TG curve in Figure 2 shows two stages of weight loss occurring at 160−600 °C. The first weight loss in a total of 5.6 wt % at 150−350 °C corresponds to the loss of the coordinated water molecules in $MnO_4(H_2O)_2$ octahedra in the lattice (calc. 5.87 wt %). The second loss of 7.3 wt % at 350−600 °C corresponds to the decomposition of DABCO molecules (calc. 8.97 wt %). XRD studies show that the

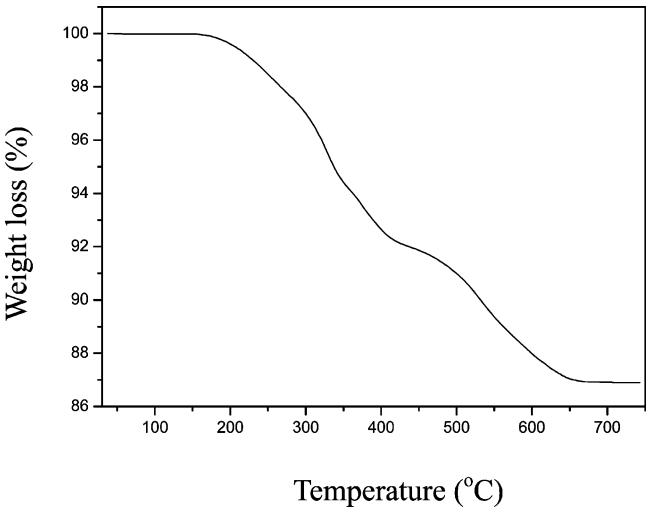

Figure 2. TG curve of MnAPO-14.

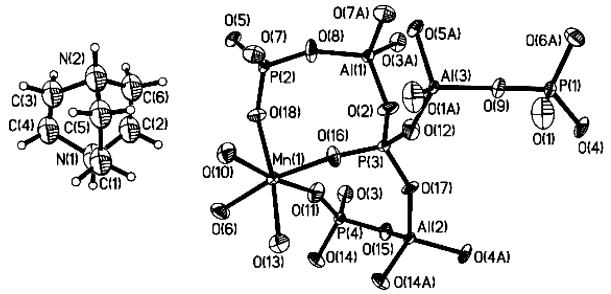

Figure 3. Thermal ellipsoid plot (50% probability) and atomic labeling scheme of MnAPO-14.

structure of MnAPO-14 collapses above 400 °C with the decomposition of the DABCO molecules.

Framework Structure of MnAPO-14. The title compound MnAPO-14 crystallizes in the $P\bar{1}$ space group with $a = 9.5121(4)$ Å, $b = 9.8819(3)$ Å, $c = 12.1172(4)$ Å, $\alpha = 70.533(2)°$, $\beta = 73.473(2)°$, $\gamma = 82.328(2)°$, and $Z = 2$. Each asymmetric unit, as can be seen in Figure 3, contains crystallographically independent Mn atom of one, Al atoms of three, P atoms of four, and DABCO molecule of 0.5. Mn (1) is six-coordinated, sharing four oxygen atoms with adjacent P atoms, with two coordinated water molecules in a cis position, forming a distorted octahedron. The average bond distance of Mn(1)−$O_{bridging}$ is 2.150(5) Å and of Mn(1)−H_2O is 2.275(5) Å, which are typical for the Mn−O bond distances of manganese phosphates.[15] Bond-valence calculation[21] results suggest that the manganese is present as Mn^{2+}. All the Al atoms are tetrahedraly coordinated by oxygen atoms connecting to P atoms. The average bond distance of Al−O is 1.736(5) Å. All the P atoms are four-coordinated to oxygen atoms, and each makes three P−O−Al bonds and one P−O−Mn bond. The P−O distances are in the range 1.486(5)−1.555(5) Å.

The linkages of $MnO_4(H_2O)_2$ octahedra, AlO_4 tetrahedra, and PO_4 terahedra through vertex oxygen atoms form the anionic open-framework $[MnAl_3P_4O_{16}(H_2O)_2]^-$, whose negative charges are compensated by diprotonated DABCO ions residing in the channels. MnAPO-14 has a zeotype AFN

(21) Brese, N. E.; O'Keefe, M. *Acta Crystallogr.* **1991**, *B47*, 192.

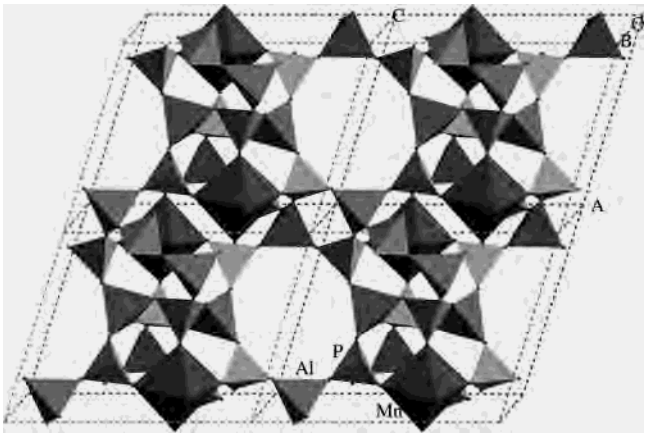

Figure 4. Framework structure of MnAPO-14 viewed along [010] direction, showing the eight-membered ring pore opening.

structure, which contains three-dimensional eight-membered ring (8-MR) channels along the [100], [010], and [001] directions, respectively. Figure 4 shows the framework along the [010] direction. The 8-MR opening is circumscribed by 4 Al atoms and 4 P atoms. Figure 5 shows an alternative view of the framework along the [001] direction. The framework of MnAPO-14 can be described by a series of 2D 4.8-net sheets connected by bridging oxygen atoms.

The diprotonated DABCO template molecules reside in the 8-MR channels (Figure 6), and form very weak H-bonds with the bridging oxygens that can be ignored, whereas strong intermolecule H-bonds are formed between diprotonated DABCO molecules with the N···N separation of 2.74(4) Å. In addition, two H_2O molecules in Mn-centered octahedron form two H-bonds to bridging oxygens with the O···O separations of 2.812 Å and 3.021 Å measured by using Cerius[2] package.

Computer Simulation of the Isomorphous Substitution of Mn(II) Atoms in AFN. The as-synthesized MnAPO-14 has a topology of zeolite AFN, in which 25% of Al atoms are replaced by octahedrally coordinated Mn(II) atoms. Replacing this Mn site by tetrahedrally coordinated Al site, denoted as Al(4), followed by energy minimization, the structure of MnAPO-14 converts to that of aluminophosphate AFN. The optimized framework $Al_4P_4O_{16}$ has a space group $P\bar{1}$ with lattice parameters $a = 9.554$ Å, $b = 9.430$ Å, $c = 10.252$ Å, $\alpha = 76.50°$, $\beta = 77.15°$, $\gamma = 84.93°$, and $Z = 2$. To understand the reason Mn(II) atom preferentially substitutes the Al(4) site instead of others, various structural models are built up through replacing individual Al sites with Mn(II) atoms followed by addition of two coordinated H_2O molecules in a cis position in Mn-centered octahedron. There are six models for each Mn-substituted site due to the different sites of the two H_2O. A total of 24 models are built up for the calculation. Two cases are considered, i.e., without and with organic amine templates occluded in the channel. Table 4 presents some calculation results that show lower framework energies and host−guest interaction energies compared with others. It is worth noting that when ignoring the guest amine template, model M1 with Mn(II) replacing Al(1) site has the lowest framework energy of −6595.60

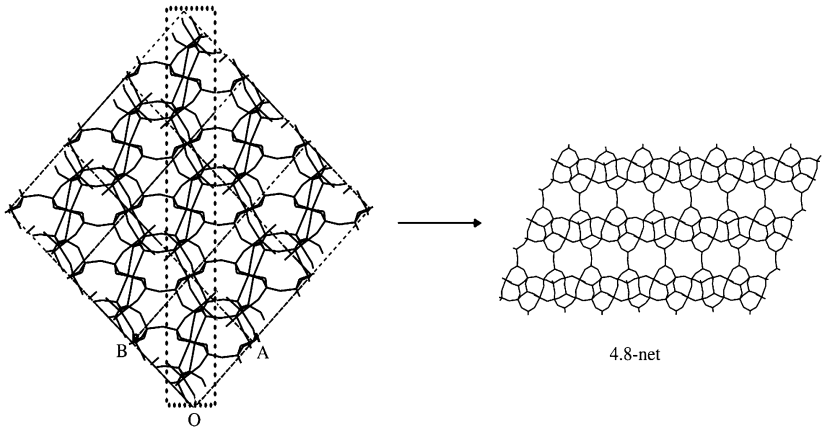

Figure 5. Framework of MnAPO-14 viewed along [001] direction (the dotted frame indicates the 2-D sheet).

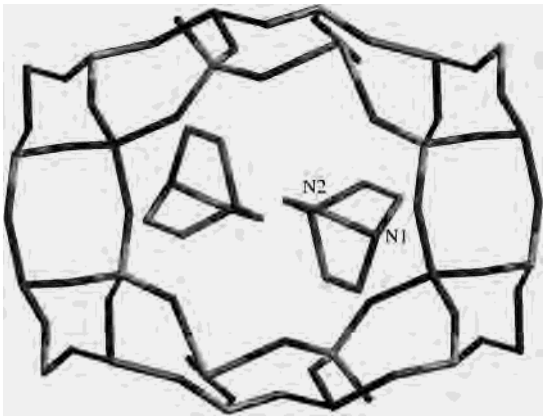

Figure 6. Diprotonated DABCO cations in the 8-MR channels.

Table 4. Calculated Energies (kcal/mol per unit cell) for Some Stable Models of Mn(II)-Substituted AFN With and Without Templates

	without template		with template	
model	substituted sites	E_f	E_{inter}	E_f
M1	Al(1)	−6595.60	−19.15	−6551.82
M2	Al(1)	−6591.81	−18.62	−6566.08
M3	Al(2)	−6583.49	−13.64	−6538.77
M4	Al(2)	−6570.23	−22.42	−6523.87
M5	Al(3)	−6584.06	−21.00	−6547.33
M6	Al(3)	−6583.28	−21.07	−6557.45
M7	Al(4)	−6582.00	−25.50	−6543.63
M8	Al(4)	−6593.86	−33.49	−6588.37

kcal/mol, whereas when taking account the guest organic amine template, model M8 with Mn(II) replacing Al(4) site shows the lowest framework energy of −6588.37 kcal/mol and host−guest interaction energy of −33.49 kcal/mol. This indicates that the host−guest interaction greatly influences the isomorphous substitution of Mn(II) atoms in AFN, which further explains the experimental substitution result in as-synthesized MnAPO-14. The optimized unit cell of M8 ($P\bar{1}$, $a = 9.595$ Å, $b = 9.768$ Å, $c = 11.989$ Å, $\alpha = 72.74°$, $\beta = 77.17°$, $\gamma = 82.49°$) is in good agreement with the experimental one of MnAPO-14; moreover, the position of the template, as well as the sites of two H_2O molecules associated with Mn-centered octahedra, is consistent with the experimental structure of MnAPO-14. Recently Stucky and coworkers[12] proposed a charge-density matching principle in which the concentrations of transition-metal atoms in the frameworks can be controlled by varying the charge and geometry of the structure-directing amine molecules.

It is believed that the substitution degree of Mn atoms in the aluminophosphate AFN framework is determined by the charge and geometry of the structure-directing DABCO molecules. This work further demonstrates that the host−guest interaction governed by the charge-density matching principle also determines the substitution sites of Mn(II) in aluminophosphate AFN topology.

Conclusions

MnAPO-14 has been synthesized hydrothermally in the presence of DABCO template molecules. The $MnO_4(H_2O)_2$ octahedra, AlO_4 terahedra, and PO_4 terahedra cross-link to form the 3-D open-framework $[MnAl_3P_4O_{18}H_4]^{2-}$ with diprotonated DABCO template molecules located in the channels compensating the negative charges. Its framework is analogous to that of aluminophosphate zeotype AFN in which 25% of the aluminum sites are replaced by Mn(II) atoms. Our work suggests that the host−guest charge-density matching principle determines not only the concentration of transition-metal ions but also the substitution sites in zeolite topology.

Acknowledgment. This work is supported by the National Natural Science Foundation of China and the State Basic Research Project of China (G2000077507).

Supporting Information Available: Crystallographic data (CIF), atomic coordinates with isotropic temperature factors, and selected bond lengths and angles for MnAPO-14 (pdf). This material is available free of charge via the Internet at http://pubs.acs.org.

IC035329A